Hierarchical Structure in LCP/PET Blends

M. S. SILVERSTEIN,* A. HILTNER, and E. BAER†

Department of Macromolecular Science and Center for Applied Polymer Research, Case Western Reserve University, Cleveland, Ohio 44106

SYNOPSIS

The structural hierarchy in injection molded blends of poly(ethylene terephthalate) (PET) and a commercial liquid crystal polymer (LCP), two immiscible polymers, was characterized at various blend compositions. The macroscopic core and skin have a gradient structure and are subdivided into ordered and disordered layers. The sublayers consist of rodlike domains at 25% LCP. The domains become thinner, longer, and more fibril-like with increasing LCP concentration. The interconnection between the LCP domains also becomes more significant at higher LCP concentrations. The highest degree of orientation in the injection direction is at the mold surface and the lowest at the sample center. The LCP orientation reflects the elongational and fountain flow in the mold and increases with increasing LCP concentration. Schematic structural models were used to illustrate the levels of structure in these blends. A minimum exists in the tensile strength, elongation at break, and impact strength with varying blend composition at approximately 50% LCP. The tensile strength of the LCP-rich blends is significantly lowered by the presence of a weldline or an angle between the stress and orientation directions. The unique mechanical properties of the LCP depend on the formation of a highly oriented and highly connected hierarchical structure that does not exist in blends with 75% or less LCP.

INTRODUCTION

Thermotropic liquid crystal polymers (LCP) have attracted a great deal of attention due to their unique mechanical properties, processing conditions, and low temperature impact. The rigid rod molecules of the polymer form a liquid crystalline phase in the molten state. The mesophase state of the liquid crystal polymer seems to consist of a polydomain texture. Each domain possesses a high degree of nematic order, an internal structure of uniform orientation. In the relaxed or annealed state there is no overall directional order among the domains themselves. The orientation of the nematic domains in the LCP can be aligned parallel to the direction of flow at quite low flow rates.[1] The alignment of the rigid rod molecules in the direction of flow yields the remarkably low viscosity of the anisotropic phase. A high level of molecular orientation is readily obtained by elongational flow at low elongational strains whereas shear strains have little effect.[2] The conditions of orienting elongational flow found during many processing operations such as film or fiber extrusion which aligns the ordered domains to a high degree in the processing direction are maintained also in the solid material.[3] The high degree of orientation yields mechanical properties such as strength, modulus, and dimensional stability (in the processing direction) that greatly surpass those of conventional polymers.

The structure of LCP processed under various conditions has been characterized extensively. A gradient solid-state structure of layers has been proposed to describe injection molded LCP.[4] A hierarchical structure with several levels of structural organization describes these layers. The structural hierarchy helps detail the architectural organization on the molecular, nano, micro, and macro levels and explains their interconnections. The rigid rod LCP molecules are arranged in fibrous interconnected microlayers, which are arranged in sublayers, which

* Present address: Department of Materials Engineering, Technion—Israel Institute of Technology, Haifa 32000, Israel.
† To whom correspondence should be addressed.

Journal of Applied Polymer Science, Vol. 43, 157–173 (1991)
 CCC 0021-8995/91/010157-17$04.00

are arranged in a macroscopic layered structure most obvious in a skin/core structure. The orientational variations in this highly complex structure were found to be directly related to the flow characteristics of the processing operation during solidification. The mechanical properties thus vary throughout the cross section of a molded LCP part due to the variation of the flow field and are highly dependent upon the processing conditions.[5] To achieve a maximum of strength and modulus in the flow direction, the highly orientable LCP would ideally be placed in an elongational flow field and cooled while in a highly ordered state. The structural hierarchy has been found in a broad range of oriented fibers, extrudates, and injection-molded articles from LCP.[6] The hierarchy in a 20 μm LCP fiber describes 5 μm macrofibrils, 500 nm fibrils, and 50 nm microfibrils.

The molecular orientation during injection molding has been modeled by coupling flow and heat transfer mechanisms with molecular theories and is well understood for thermoplastic materials.[7] Shear flow behind an advancing fountain flow front in the mold is combined with extentional flow and a solidified layer highly oriented in the direction of flow at the cold wall of the mold. This knowledge can be readily applied to a thermotropic LCP in order to understand its flow behavior during injection molding through the orientation distribution in the molded part. The skin/core layered structure and the parabolic arcs in the core observed in the structural studies of the injection-molded LCP cited above clearly reflect the flow patterns in the mold. The highly oriented structure and superior mechanical properties of the skin result from the elongational flow of the LCP at the cold wall of the mold. The shear flow at the center yields unoriented LCP without the superior mechanical properties of the oriented material. A weldline in an injection molding at the meeting of two fountain flow fronts yields orientation perpendicular to the main flow direction and thus a weak point for an anisotropic rigid rod LCP.[8] The number of layers and their orientation depends on sample geometry and processing conditions. In general there is a highly ordered top layer and a nonoriented core layer while the layers between them can have various degrees of orientation.

Glass-fiber-filled LCP composites were studied in order to characterize the effects of the fibers upon the properties of the LCP. The orientation of the glass fibers in the injection-molded composites was similar to the orientation of the neat LCP and followed the familiar fountain flow pattern. The inclusion of these inadequately adhering fibers in the LCP matrix yielded composite materials with a lower tensile strength than the neat LCP.[9] The LCP fractured in a woodlike manner during the cyclic loading of a notched specimen with delocalized zig-zag crack propagation. In the fiber reinforced LCP the localized fracture path was somewhat zig-zag in nature but was largely confined to the plane of the notch.[10] The presence of the glass fibers interfered with the highly connected hierarchical LCP structure that yields the unique material properties.

There has been an interest in LCP blends since blending a thermotropic LCP with a thermoplastic might yield a self-reinforcing polymer under the right processing conditions. The self-reinforcing polymer blend would have LCP fibrils reinforcing a thermoplastic matrix. One advantage of the self-reinforcing polymer blend over traditional fiber-reinforced thermoplastic composites would be the low viscosity of the blend. The low viscosity of the LCP would tend to lower the processing viscosity of the blend while the viscosity of thermoplastics is increased by glass fiber reinforcement. Additionally the wear on processing equipment associated with glass-fiber-filled thermoplastics would be eliminated by the self-reinforcing polymer blend. A variety of LCP/thermoplastic blends were studied yielding a multitude of often conflicting results. The studies on these blends used different materials, compositions, and processing conditions. The blend morphology is, however, highly processing and composition dependent in these blends. The properties of the blends, intimately related to their structure, are therefore also highly dependent upon these parameters. It is anticipated that the compatibility of the LCP with the thermoplastic material, the interphase adhesion in these phase separated systems, is another significant factor which determines the structure, and thus the properties, of the blend systems.

In general, at low LCP concentrations, LCP spheres, cylinders, and fibrils were observed with increasing LCP concentration and increasing prominence of elongational flow in the system.[11] At higher LCP concentrations (above 50%) phase inversion was observed with the LCP becoming the matrix polymer.[12] The elongational flow was related to the orientation of the LCP and the properties of the blends. The strength and modulus in the flow direction increased with increasing LCP concentration and orientation.[13] The rheological behavior of the blends in the mold is complicated by the different viscosities of the components and the variation of the flow conditions through the mold thickness. These flow parameters, of course, are themselves dependent on the processing conditions and composition.

The purpose of this research is to fully characterize the structure in blends of a thermotropic LCP with poly(ethylene terephthalate). The effects of blending upon the LCP hierarchical structure, the resulting blend domain structure, and the relationship between the structure and the properties will be determined. In this study the relationship between the blend composition and the 3-dimensional structure is characterized. Structural models are developed to better describe the resulting complex superposition of the LCP hierarchical structure on the domain structure in the blends. The mechanical properties of the blends are evaluated to define the relationship between the structure and properties in these blends. The 3-dimensional characterization of the blends' complex hierarchical-domain structure and its relationships to the processing conditions and the blends' mechanical behavior in this study should serve as a model that could be extended to similar self-reinforcing polymer blend systems.

EXPERIMENTAL

The injection-molded LCP/PET blends were supplied by Goodyear Tire and Rubber Co. The PET for the blends was supplied by Goodyear, and the LCP for the blends was Vectra A-900, an aromatic copolyester [copolymer of hydroxybenzoic acid (HBA) and hydroxynaphthoic acid (HNA)], supplied by Hoechst Celanese Corp. The LCP/PET blends were of the following compositions: 0, 5, 25, 50, 75, 95, and 100 wt % LCP. The neat polymers were blended at 285°C with a 1-in. single screw extruder and then pelletized. The blend pellets were then injection molded at 290°C with a mold temperature of 27°C. The mold used was either an ASTM cluster or a 15 cm × 15 cm × 0.3 cm plate.

The 0.9 mm thick plaque specimen from the ASTM cluster was chosen as the subject for the morphological analysis. A strip 3 mm wide was cut from the middle of the bottom edge to the center of the plaque opposite the inlet sprue at the middle of the top edge of the plaque. The cross section of the center cut from the bottom edge is a cross section perpendicular to the direction of flow, as illustrated schematically in Figure 1. A second strip 3 mm wide was cut from the middle of the side edge to the center of the plaque. The cross section of the center cut from the side edge is a cross section in the direction parallel to the direction of flow. These cross section specimens were microtomed to 0.5 μm thick samples with a diamond knife. The microtomed sections were viewed through crossed polars in transmission optical microscopy (TOM) using an oil immersion technique with a × 100 lens.

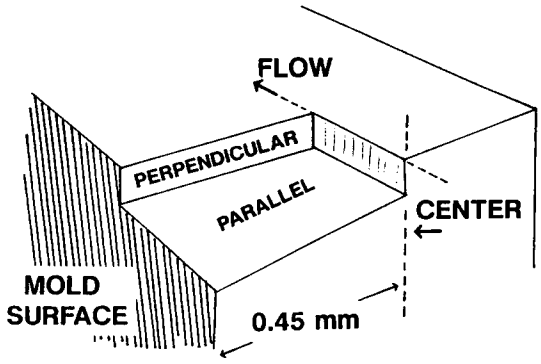

Figure 1 Schematic diagram depicting the sections of the injection molded sample used for structural characterization.

These strips 0.5 μm thick, 0.9 mm wide, and 3 mm long were viewed across their width to include the entire thickness of the injection molded specimen. The microtomed surfaces of the thickness cross section sample strips from the bottom and side edges were then etched in preparation for the scanning electron microscope (SEM). The PET in the blends was etched from the microtomed surface of the strip using a reagent grade 40% methylamine aqueous solution supplied by Fisher Scientific. The surface of the strips was immersed in the etching solution overnight. The etched surface was washed, first with dimethyl sulfur dioxide (DMSO) and afterwards with water, and then dried in air at room temperature. The entire thickness cross section was examined at low magnification and the sample edge and center at higher magnification.

To complete the 3-dimensional characterization of the blend the structure of the plaque was also examined with sections through the thickness. The plaque was polished in the thickness direction with sandpaper to a specific depth. The exposed surface was then polished with fine alumina powders to remove scratches. One plaque was polished approximately 30 μm to expose the skin layer, just below the mold contact surface, or top layer. Another plaque was polished 0.45 mm to expose the center of the 0.9 mm thick sample. The PET in the top layer, skin layer, and central layer were etched with 40% methylamine as described above. The etched layers were examined in the scanning electron microscope. The results of these microscopic analyses in the three perpendicular directions were the basis for the construction of a schematic structural model. These models were created in order to more fully

describe these blends and illustrate the influence of composition and processing upon the structure.

The mechanical properties of the injection-molded blends were characterized through tensile testing on an Instron tensile testing machine. Injection-molded dogbone samples were tested in the injection direction at room temperature at a strain rate of 1%/min. A second series of tensile specimens were injection molded with weldlines at the center of the dogbone. A weldline at the center of the specimen was introduced by opening the inlet gates at both ends of the specimen mold. The effect of the LCP orientation on the mechanical properties was determined through tensile tests on dogbone specimens cut from injection molded plaques. These specimens were cut such that the tensile direction would be at approximately 45° from the injection direction. The tensile modulus, tensile strength (or yield strength in ductile samples), and elongation at break (or elongation at yield for ductile samples) were used to characterize the effects of blend composition, weldlines, and sample orientation on the mechanical behavior of the blends. Izod impact specimens were taken from injection-molded flexure bars which were cut in half and notched. The specimens were categorized by their composition and the relative distance of the notch from the inlet sprue at the top of the flexure bar. The results of the tensile tests represent 6–10 specimens and the results of the impact tests represent 12–20 specimens.

Differential scanning calorimetry (DSC) was used to characterize the glass, melt, and crystallization transitions of the blends. Samples for the DSC were taken from the 0.9 mm thick plaques used for the structural analysis and included the entire thickness. The samples were run from room temperature until 320°C at 20°C/min three times. The first cooling rate, between the first and second heating, was 40°C/min for a rapid cool. The second cooling rate, between the second and third heating, was 10°C/min for a slow cool. The temperature, breadth, and heat of the transitions were examined for the various blend compositions for all five runs.

RESULTS AND DISCUSSION

Morphology

LCP

The LCP structural characterization at various size scales has revealed a hierarchical structure in previous studies. The injection-molded neat LCP exhibits a complex structure on even the macroscopic level. The reflection optical micrograph in Figure 2 of a polished surface of an LCP plaque 0.9 mm thick cut parallel to the injection direction (as described in Fig. 1) reveals the complex structure through changes in color across the specimen thickness. At even low magnification a skin layer approximately 0.3 mm thick is observed at the mold contact surface of the plaque. There is a distinct top sublayer at the mold surface on the order of tens of microns within the skin layer which can also be distinguished by its color. A core layer approximately 0.3 mm thick is also seen in Figure 2. Within the core layer there is a central sublayer approximately 0.15 mm thick. To elucidate the reason for these distinct layers on the macroscopic level, the structure at the microscopic level is examined.

The surface, viewed optically in Figure 2, is seen in an SEM micrograph in Figure 3(a). Skin and core layers can be distinguished through their distinctive flow patterns. The skin and core are each approximately one third of the specimen thickness, 0.3 mm, as described in the optical micrograph of Figure 2. A higher magnification near the mold surface, in Figure 3(b), reveals LCP fibrils on the order of 1–2 μm in diameter. These LCP fibrils near the mold surface are highly oriented in the injection direction. A higher magnification at the center of the sample, in Figure 3(c), also reveals LCP fibrils 1–2 μm in diameter. The fibrils at the center, however, are oriented in a distinctive parabolic flow pattern.

The orientation pattern of the LCP in the injection-molded plaque is a result of the flow field during

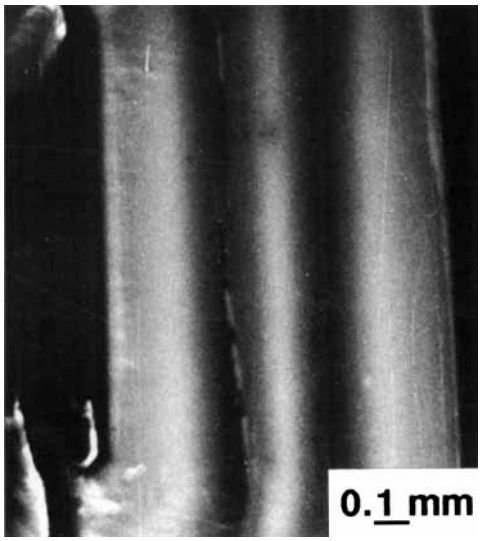

Figure 2 Reflection optical micrograph of LCP cross section parallel to injection direction (× 100)

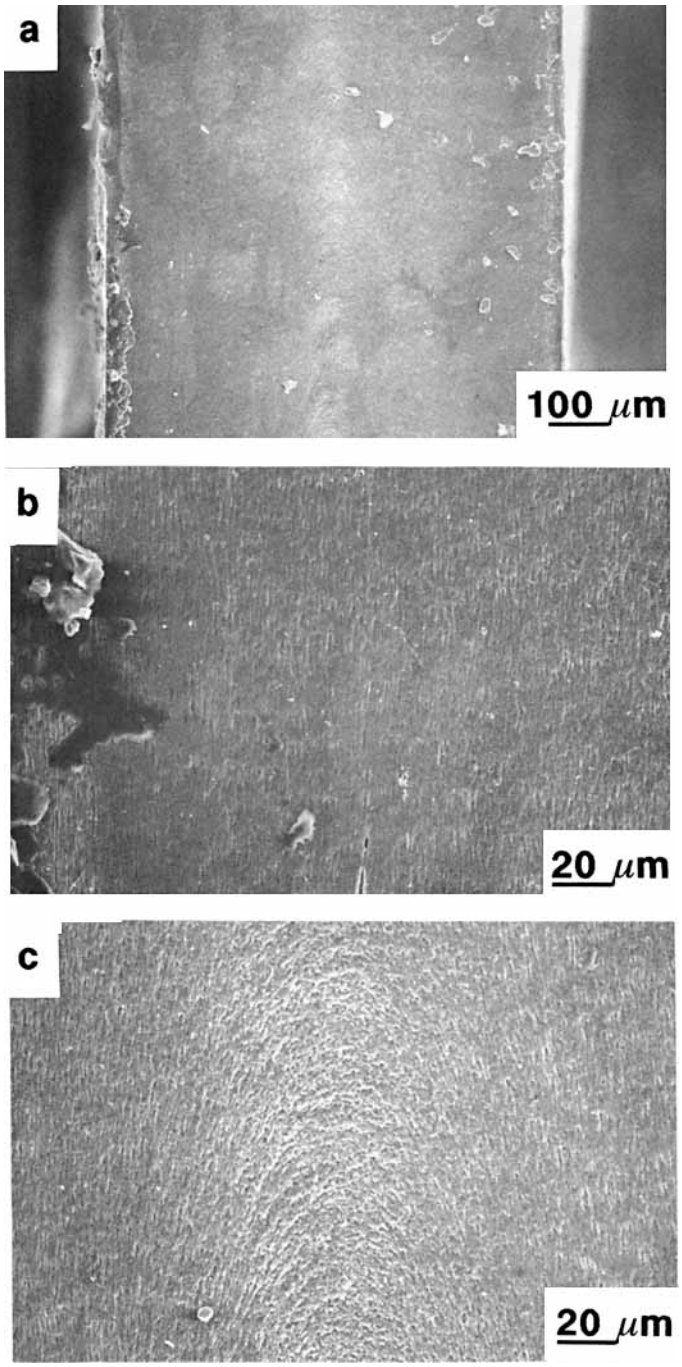

Figure 3 SEM micrograph of LCP cross section parallel to injection direction: (a) × 100; (b) sample edge, × 500; (c) sample center, × 500.

molding. The elongational flow in the injection direction at the cold mold surface yields an oriented skin layer. The fountain flow in the plaque center yields a core layer with a distinct parabolic arc orientation of the LCP fibrils. This skin/core effect is well documented in injection-molded thermoplastics and is of great significance in thermotropic LCP owing to their low viscosity and high orientability. The change in orientation through the sample thickness generated by the flow pattern yields the color changes in the molded LCP that can be distinguished with the naked eye. The complex hierarchical structure in injection molded LCP has been detailed in other studies.[4,6]

50% LCP Blend

The characterization of the blends must also detail the structure on various size scales in order to understand the superposition of a blend domain structure upon the LCP hierarchical structure. A section parallel to the injection direction (as indicated in Fig. 1) of a 50% LCP blend in the reflection optical micrograph in Figure 4 exhibits a barely discernable change in color. The macroscopic change indicates the existence of a skin and core in the 50% LCP blend. The skin/core structure from Figure 4 is not as distinct as that of the neat LCP in Figure 2. The color change in the 50% LCP blend is gradual and the boundaries between the skin and core layers are not as sharply defined. The top sublayer and central sublayer, which could be easily distinguished in the neat LCP, are difficult to discern in the 50% LCP blend.

A 1 μm thick section microtomed from the surface of the sample in Figure 4 is seen in Figure 5, using transmission optical microscopy with crossed polars. The LCP domains in Figure 5 are easily distinguished from the transparent PET. The micrograph montage depicts half the cross section of the sample, from the plaque's edge or mold surface to its center. Five sublayers can be approximately distinguished in these micrographs through differences in the size, shape, and orientation of their LCP domains. There is, however, no distinct border between the sublayers but rather a gradual change in the size, shape, and orientation of the LCP domains from sublayer to sublayer.

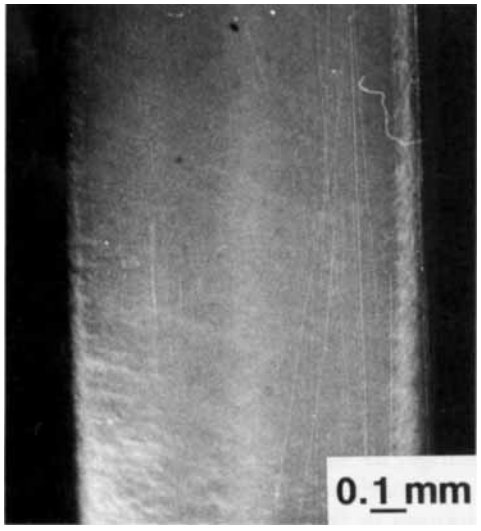

Figure 4 Reflection optical micrograph of 50% LCP blend cross section parallel to injection direction (× 100).

The first sublayer or top sublayer (from 0 to 1 on the bottom of the micrograph), approximately 20 μm thick at the mold surface, consists of elongated fibrillar LCP domains 1–2 μm in diameter. These LCP fibrils are highly oriented in the injection direction. The sublayer next to the top layer (1 to 2) is approximately 120 μm thick. This second sublayer consists of cylindrical LCP domains 2–5 μm in diameter oriented in the injection direction. These LCP domains are shorter, thicker, and less oriented than those in the top layer. The third sublayer (2 to 3) is also approximately 180 μm wide and has still shorter, thicker, and less oriented LCP domains. The LCP domains in the fourth sublayer (3 to 4), approximately 100 μm wide, are similar to those in the third sublayer but are somewhat more oriented in the injection direction. The fifth or central sublayer (twice the distance from 4 to 5 at the sample center), approximately 60 μm wide, has short, thick LCP domains that seem to be oriented in a direction perpendicular to that of the injection direction.

A 1 μm thick microtomed section of the 50% LCP plaque cut perpendicular to the injection direction (as indicated in Fig. 1) yields further insight into the LCP structure. Figure 6 is a transmission optical micrograph from the center of the sample. The LCP domain structure perpendicular to the injection direction is identical from edge to center. The entire cross section consists of globular LCP domains 2–5 μm in size with no particular orientation and no distinguishable layered structure. Perpendicular to the injection direction the LCP domains at the plaque's edge cannot be distinguished from those at its center. The structural organization of the LCP is dependent upon the flow during processing and reflects the flow field in the mold. The extensional flow in the injection direction in the mold is thus reflected in the rodlike LCP microdomains with their major axis oriented in the injection direction. This microdomain orientation can thus be observed in the sample cut parallel to the direction of flow, but cannot be observed in the sample cut perpendicular to the injection direction.

The same surface parallel to the injection direction seen in Figures 4 and 5 is seen in the SEM micrograph in Figure 7(a). The PET has been etched leaving behind a distinct LCP structure on the surface. The LCP domains are, in general, oriented in the injection direction. A skin-core structure is also obvious in Figure 7(a). The LCP domains at the sample center are arranged in a parabolic arc approximately 80 μm wide. The parabolic arc for the 50% LCP blend is about half the size of

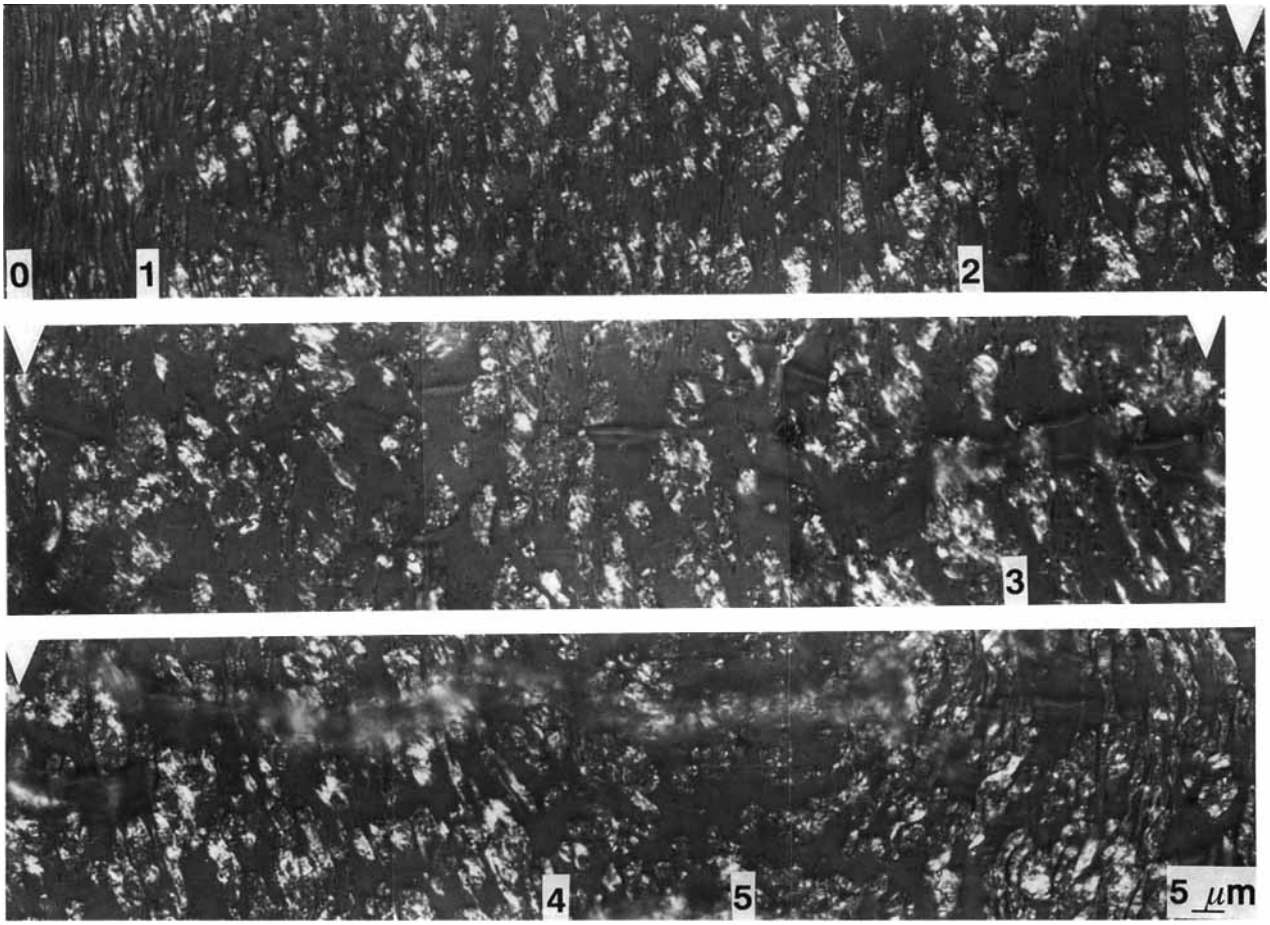

Figure 5 Transmission optical micrograph of 50% LCP blend cross section parallel to injection direction (× 2000): (0) sample edge; (1) end of 1st sublayer; (2) end of 2nd sublayer; (3) end of third sublayer; (4) end of 4th sublayer; (5) sample center. White triangles identify identical areas on the first and second micrograph strips and on the second and third micrograph strips.

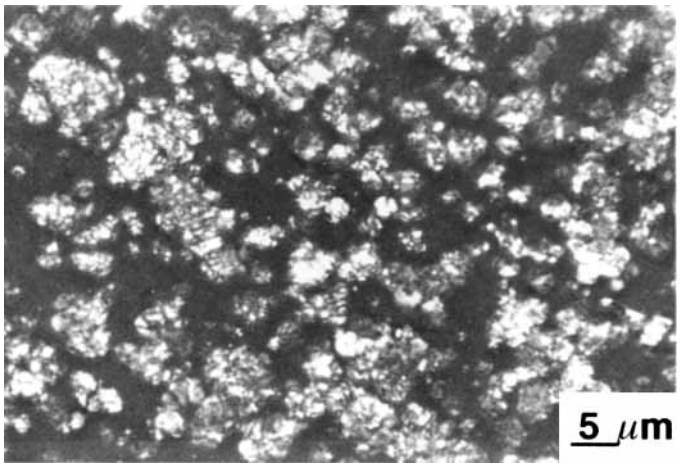

Figure 6 Transmission optical micrograph of 50% LCP blend cross section perpendicular to injection direction (× 2000).

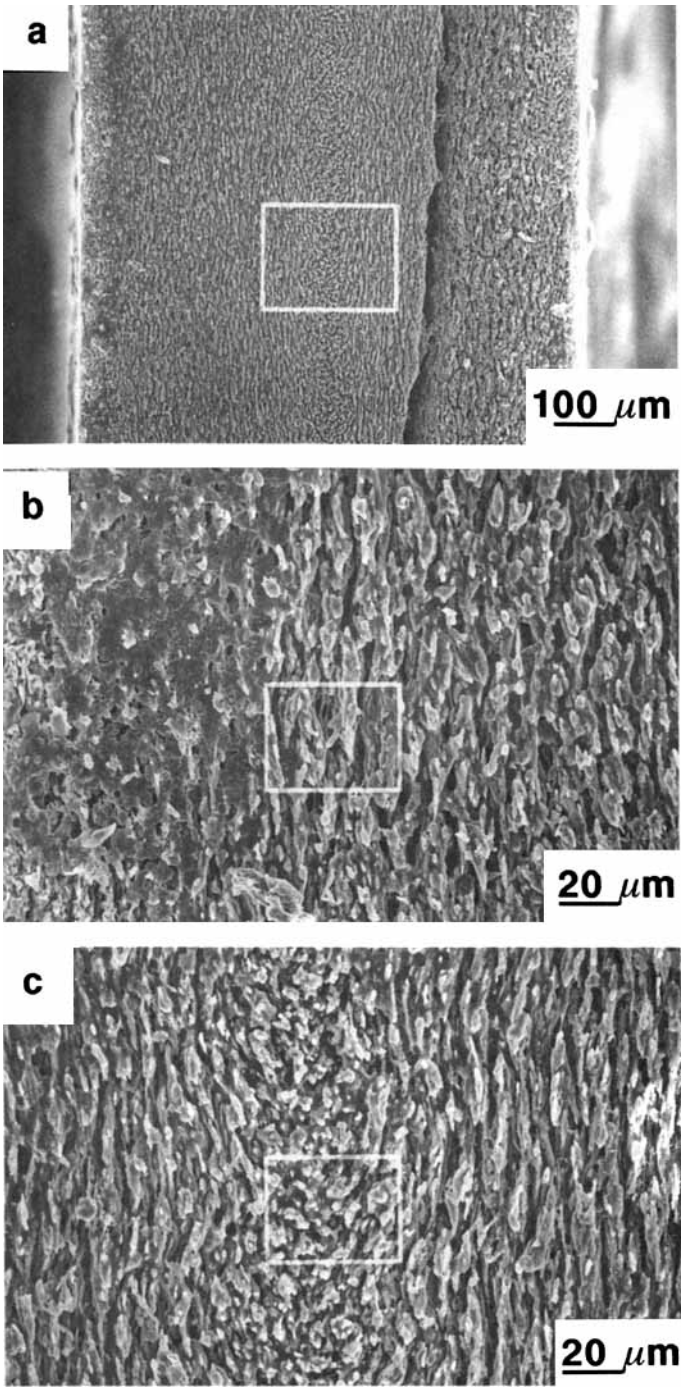

Figure 7 SEM micrograph of 50% LCP blend cross section parallel to injection direction: (a) × 100; (b) sample edge, × 500; (c) sample center, × 500.

that for the LCP seen in Figure 3(b). Figure 7(b), a higher magnification of the edge of the sample in Figure 7(a), reveals cylindrical LCP domains 2–5 μm in diameter and tens of microns in length, oriented in the injection direction. These cylindrical domains seem to be organized in interconnected microlayers in the injection direction. The LCP domains at the center of Figure 7(a), seen at higher magnification in Figure 7(c), have the same diameter as those near the edge but are not orientated

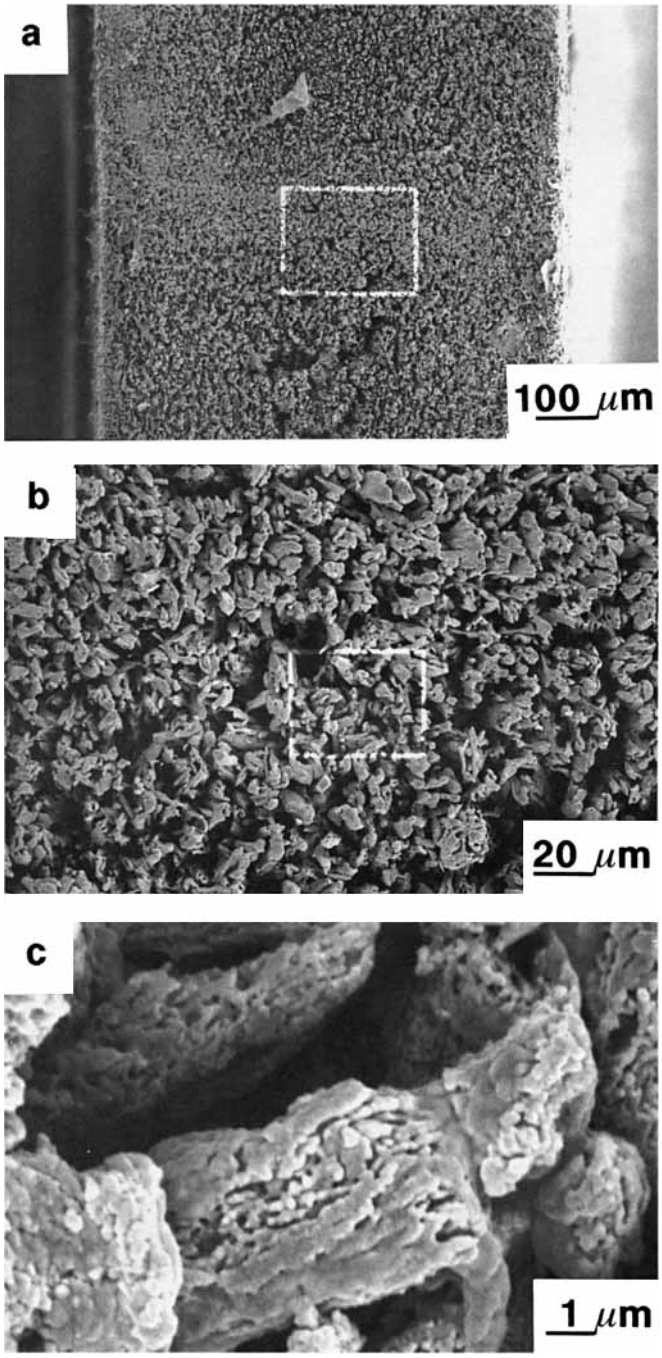

Figure 8 SEM micrograph of 50% LCP blend cross section parallel to injection direction: (a) × 100; (b) sample center, × 500; (c) sample center, × 10,000.

in the injection direction. The parabolic arc orientation of the LCP at the center is difficult to discern at high magnification.

The SEM micrograph in Figure 8(a) of an etched sample cut perpendicular to the injection direction (as indicated in Fig. 1) has no discernable layered structure. In Figure 8(a) the LCP domains at the sample's edge are similar in size, shape, and orientation to those at the sample's center, seen at higher magnification in Figure 8(b). These domains, 2–5 μm in diameter, seem to be part of a structure which extends perpendicular to the micrograph. Higher

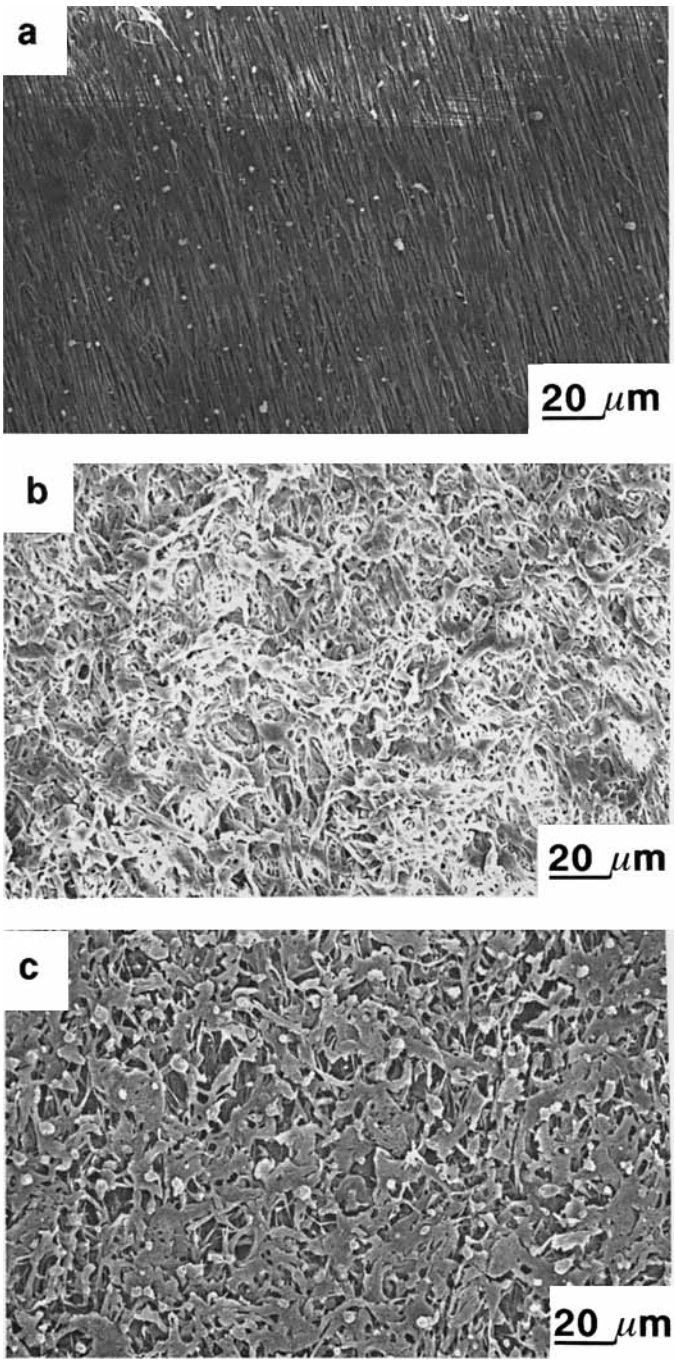

Figure 9 SEM micrograph of 50% LCP blend (× 500): (a) top microlayer; (b) skin microlayer; (c) central microlayer.

magnification in Figure 8(c) reveals that the 2–5 μm diameter domains are themselves constructed of submicron LCP microdomains tenths of microns in diameter. The description of the structure through SEM characterization supports that from optical microscopy. The microdomains form domains; the domains form microlayers; the microlayers form sublayers; and the sublayers form a layered structure. This organization from microdomains to a layered structure is the structural hierarchy in the 50% LCP blend.

A third direction, perpendicular to the two examined thus far, will elucidate further the structure within the microlayers. The microlayers are the lay-

ers which together form the sublayers characterized in the previous analyses. The mold contact surface with the PET etched in Figure 9(a) reveals a microlayer of the top sublayer. This microlayer consists of highly oriented LCP fibrils 1–2 μm in diameter. These fibrils are highly connected within the microlayer as well as being connected to neighboring microlayers. The microlayer in Figure 9(b) lies beneath the top sublayer, with approximately 30 μm, 3% of the total thickness, removed by polishing. This skin microlayer is composed of an entangled network of fibrils and clumps of fibrils approximately 2–5 μm in diameter. This microlayer is also highly intraconnected (within the microlayer) as well as being interconnected (with neighboring microlayers). There is an overall orientation direction to the networklike layer which is not easily discernable and resembles a fishing net stretched in uniaxial tension. The microlayer in Figure 9(c) is from the central sublayer with 50% of the thickness removed by polishing. There is no obvious orientation in this central microlayer, with 2–10 μm more platelike than fibrillar LCP domains. The central microlayer is extensively intraconnected as well as being interconnected. The differences between the structure at these various positions through the sample cross section is highlighted by the very different microlayers in Figure 9.

A 3-dimensional picture of the 50% blend can be constructed from the optical and electron micrographs which have revealed various parts of the structural hierarchy. The 20 μm top sublayer is highly oriented consisting of LCP fibrils 1–2 μm in diameter arranged in intraconnected microlayers. The skin and core layers contain sublayers each of which is constructed of cylindrical LCP domains 2–5 μm in diameter. The oriented LCP structures in the first two sublayers result from the elongational flow in the injection direction along the cold mold surface. The central sublayer consists of larger more platelike LCP domains bearing no specific orientation but arranged in a parabolic arc. The peak of the parabola at the sample's center results from shear fountain flow. The microlayer is not only connected within itself but is also connected to neighboring microlayers.

The resulting disrupted LCP structure in the 50% LCP blend is illustrated schematically in Figure 10. There are layers, sublayers, and microlayers from edge to center, each with LCP domains of a distinctive size, shape, and orientation. LCP domain structures typical to the top (A), second (B), and central (C) sublayers have been enlarged in 3-dimensional sketches. The schematic model highlights

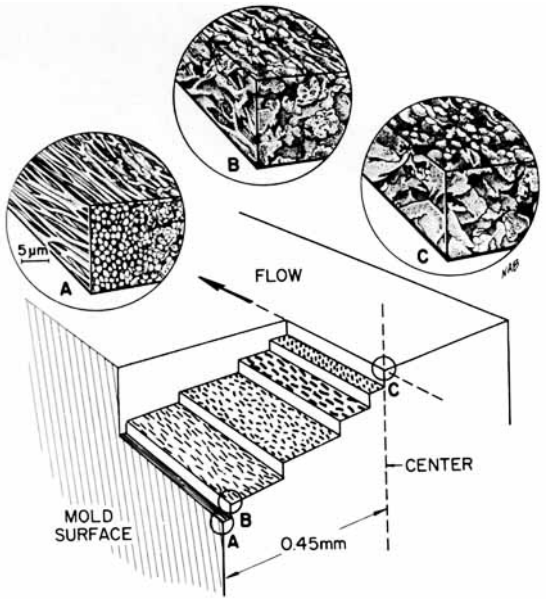

Figure 10 Schematic illustration of the hierarchical structure in 50% LCP blend. LCP domains arranged in five sublayers. A top microlayer (A), skin microlayer (B), and central microlayer (C) are illustrated at higher magnification.

the various levels observed in the blend's hierarchical structure and illustrates the effects of the flow conditions upon the final LCP structure at different positions in the cross section. The PET matrix surrounds the LCP domains throughout the blend. The PET affects the LCP structure through changes in the flow field during processing and through polymer incompatibility. There is a smaller degree of orientation in the blends than in the LCP due to the presence of the more viscous and less orientable PET. The incompatibility of the LCP and PET limits the extent to which the LCP can develop a connected structure. The hierarchical 3-dimensional highly oriented and connected structure of LCP fibrils in the neat LCP is disrupted by the PET in the blend.

75% LCP Blend

The LCP/PET blend with 75% LCP has been structurally analyzed in the same manner as the 50% LCP blend. This combination of optical and electron microscopy in different directions has yielded a graphic description of the structures of all the blends. The edge of an etched 75% LCP blend sample cut parallel to the injection direction (as described in Fig. 1) is seen in Figure 11. LCP fibrils, 2–5 μm in diameter, are highly oriented in the injection direc-

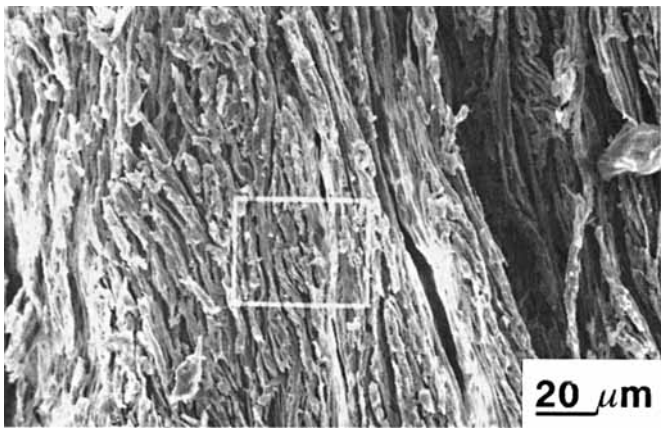

Figure 11 SEM micrograph of 75% LCP blend cross section parallel to injection direction at sample edge (× 500).

tion in the skin. The fibrils are longer, slightly thinner, and more closely packed than those seen in Figure 7(b) for the 50% LCP blend. The LCP domains at the center (not shown) are, as in the 50% blend, oriented in a parabolic arc. The LCP structure perpendicular to the injection direction (not shown) reflects the existence of a fibrillar structure perpendicular to its surface. In general, the SEM and TOM micrographs indicate the existence of a structure in the 75% LCP blend that is similar to that of the 50% LCP blend. The etched microlayer from the top sublayer in Figure 12(a) has highly oriented branched LCP fibrils more closely packed, intraconnected, and interconnected than the fibrils in the 50% LCP blend. A skin microlayer, 0.3 μm beneath the top microlayer, exhibits plumed LCP domains oriented in the injection direction in Figure 12(b).

The structure of the 75% blend as determined through microscopy is illustrated schematically in Figure 13. There are approximately six sublayers in the structure that can be distinguished through the size, shape, and orientation of the LCP domains. The microlayer in the top sublayer (A) consists of highly connected and oriented branched fibrils. The second sublayer (B) consists of plumed LCP domains whose general orientation is in the injection direction. The central sublayer (C) consists of closely packed shorter LCP domains arranged in a parabolic arc whose peak is at the plaque's center. The overall structure is similar to that of the 50% blend. The varying size, shape, and orientation of the LCP domains through the sample cross section follows the flow field pattern. The LCP has more continuity in the 75% blend since it is the major component. The hierarchical highly oriented and connected structure typical of neat LCP is disrupted by the PET in the 75% LCP blend.

25% LCP Blend

The structure of the 25% LCP blend follows the pattern observed in the 50% and 75% LCP blends. The micrograph in Figure 14 is the edge of the etched 25% LCP blend surface cut parallel to the direction of flow (as described in Fig. 1). LCP fibrils 2–5 μm in diameter can be distinguished in this blend both at the edge of the sample and at its center (not shown). Near the center there is a slight parabolic arc orientation. The boundaries between the sublayers in the 25% blend are difficult to discern. Three sublayers can be defined with a highly oriented top sublayer in an oriented skin layer and a less oriented core layer that includes a slight parabolic orientation near the center. The structure of the 25% LCP blend is depicted schematically in Figure 15. The microlayer in the top sublayer (A) consists of highly oriented LCP fibrils. The microlayer in the second sublayer (B) consists of short cylindrical LCP domains with a general orientation in the injection direction. The central microlayer (C) consists of cylindrical LCP domains oriented perpendicular to the injection direction. Near the center the LCP domains are arranged in a parabolic arc. The LCP domain structure reflects the flow pattern during processing. The elongational flow at the mold surface yields the highly oriented fibrils. The fountain flow yields short discontinuous cylindrical LCP domains oriented in a pattern described in the literature for glass fibers in a thermoplastic matrix.

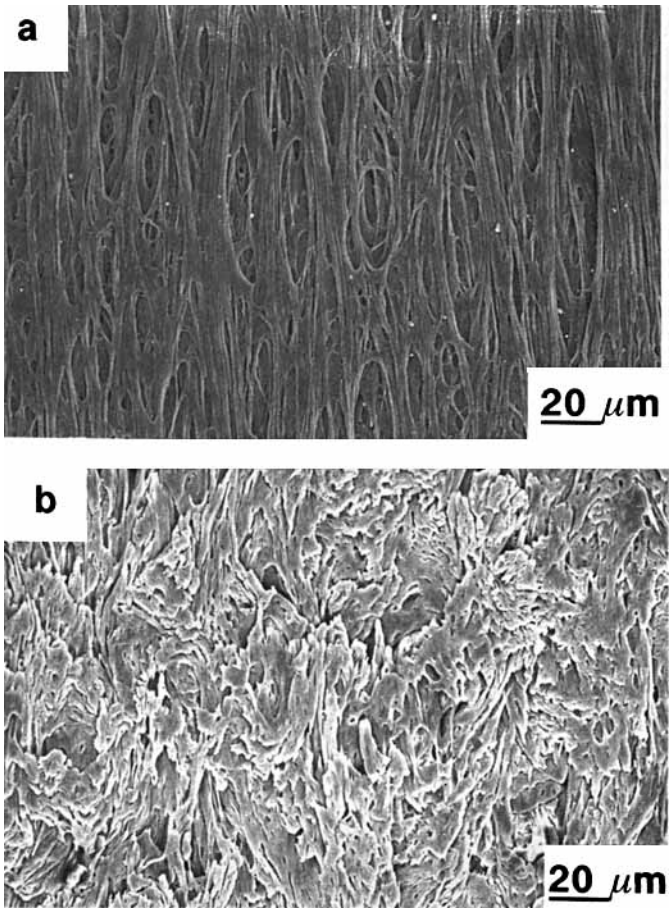

Figure 12 SEM micrograph of 75% LCP blend (× 500): (a) top microlayer; (b) skin microlayer.

5% LCP and 95% LCP Blends

The structure of the blend with 5% LCP is that of spherical LCP domains in a PET matrix, as seen in the transmission optical micrograph in Figure 16. The addition of 5% LCP to the transparent PET matrix yields an opaque blend. The spherical domains are found both at the edge and at the center, throughout the cross section, in directions both parallel and perpendicular to the injection direction. This particle inclusion in a continuous matrix structure found in the 5% LCP blend with a PET matrix is also found in the 95% LCP blend. In the 95% LCP blend there is an LCP matrix and spherical PET inclusions. The micrographs of an etched 95% LCP blend surface (not shown) reveal a cratered LCP matrix from which the spherical PET particles were etched.

The structure in the blends thus changes from an LCP particulate filled PET at 5% LCP to an LCP short fibril filled PET at 25% LCP. At 50% LCP in the blends the oriented microlayer mats of cylindrical LCP domains become connected. The microlayer connections increase with the amount of LCP in the blend. The hierarchical highly connected structure typical of neat LCP is already developed in the 95% LCP blend, with 5% PET spherical inclusions in the LCP matrix.

Differential Scanning Calorimetry

Differential scanning calorimetry was used to determine the transition temperatures in the blends. The first cycle, heating at 20°C/min, revealed a glass transition (approximately 75°C), a crystallization (approximately 125°C), and a melting (approximately 250°C) all ascribable to the PET. One LCP transition (approximately 260°C) was also revealed in the initial heating. Slow cooling the blends at 10°C/min revealed a PET crystallization transition. Reheating at 20°C/min revealed a PET melting

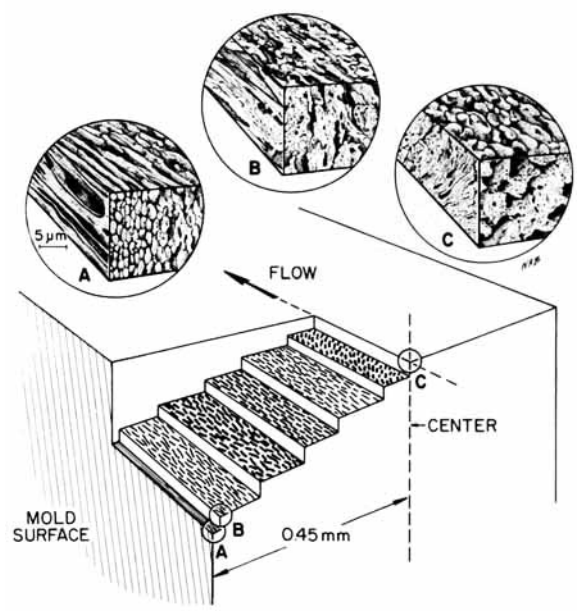

Figure 13 Schematic illustration of the hierarchical structure in 75% LCP blend. LCP domains arranged in six sublayers. A top microlayer (A), skin microlayer (B), and central microlayer (C) are illustrated at higher magnification.

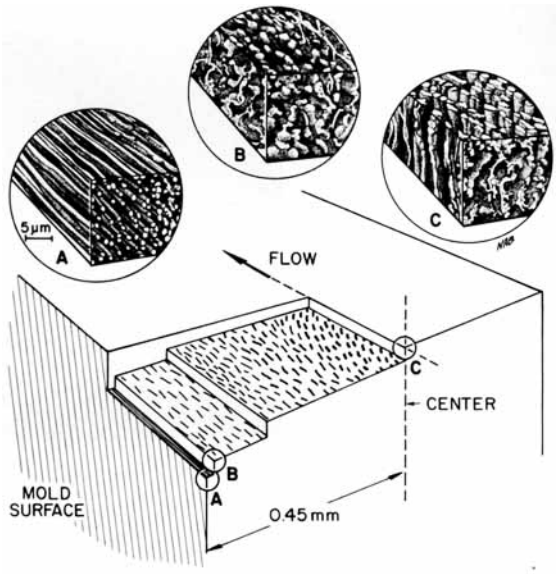

Figure 15 Schematic illustration of the hierarchical structure in 25% LCP blend. LCP domains arranged in three sublayers. A top microlayer (A), skin microlayer (B), and central microlayer (C) are illustrated at higher magnification.

transition. The variation of these six transitions with temperature are seen in Figure 17. The three transition temperatures of the amorphous PET during the initial heating are relatively unaffected by the presence of the LCP. The LCP transition temperature is unaffected by the amount of PET. The crystallization of the PET upon slow cooling, however, is impeded by 75% or more LCP. The LCP restricts the mobility of the PET, the minor component, and the crystallization temperature decreases. The crystallization temperature decreases by 50°C at 75% or more LCP and the melting temperature upon reheating is also reduced. There is no evidence of significant transesterification or molecular mixing between the PET and LCP. The two immiscible polymers are phase separated into the previously described structures.

Mechanical Properties

The variation of the mechanical properties with the amount of LCP in the blends is a direct consequence

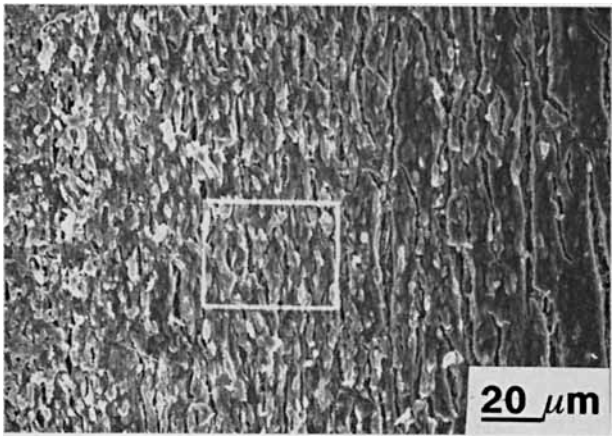

Figure 14 SEM micrograph of 25% LCP blend cross section parallel to injection direction at sample edge (× 500).

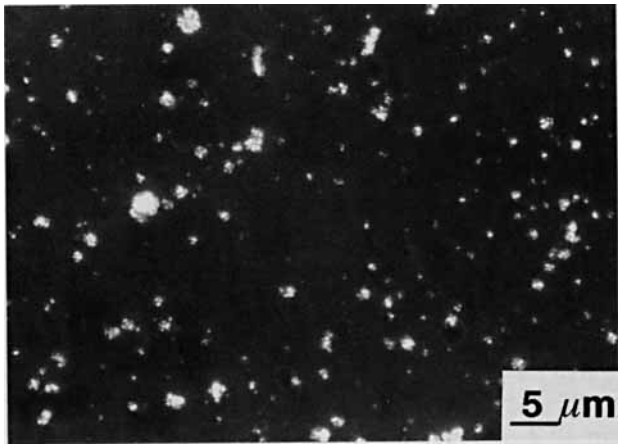

Figure 16 Transmission optical micrograph of 5% LCP blend cross section parallel to injection direction (× 2000).

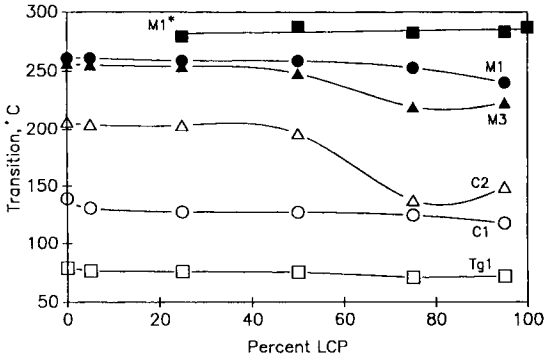

Figure 17 Variation of transition temperatures with composition in the PET/LCP blends. Initial heating (20°C/min): T_{g1} = PET glass transition; C_1 = PET crystallization; M_1 = PET melting; M_1^* = LCP transition. Cooling (10°C/min): C_2 = PET crystallization. Second heating (20°C/min): M_3 = PET melting.

of the variation in their structure. The stress–strain curves in Figure 18 illustrate the differences between the PET, LCP, and their blend in equal proportions. The PET has a yield stress and draws. The 5% LCP blend behaves in the same manner, consistent with an LCP particulate filled PET matrix structure. The LCP exhibits a high modulus and a high strength. The LCP fracture surface is jagged, similar in texture to that of wood. It is the woodlike nature of the LCP that makes it a tough material. The 50% LCP blend, however, has a significantly lower strength and strain to break than either of the component polymers. The fracture in the 50% LCP blend is brittle, with neither PET-like drawing nor woodlike fracture. The mechanical behavior reflects the structure in the 50% LCP blend. There is too much LCP to allow PET-like drawing, but not enough LCP to form a highly connected tough hierarchical structure.

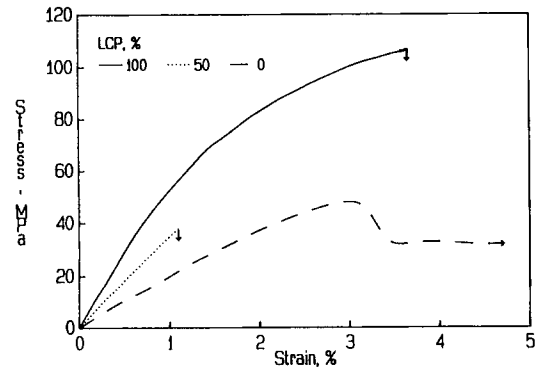

Figure 18 Stress–strain curves of PET, 50% LCP blend, and LCP (strain rate, 1%/min). No weldline.

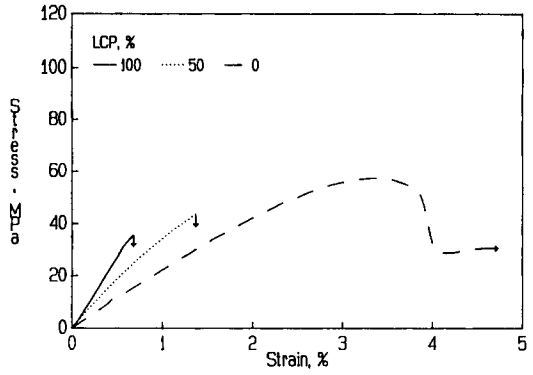

Figure 19 Stress–strain curves of PET, 50% LCP blend, and LCP (strain rate; 1%/min). Weldline in center.

The LCP sensitivity to weldlines in the molded part is illustrated in Figure 19, where the PET is seen to be relatively weldline insensitive. The PET can entangle and mesh across the weldline where the two flow fronts meet. The loss of strength in the LCP is due to the presence of a weak point at the weldline. The weak point created by a weldline in the LCP is due to the absence of the highly oriented and connected structure across the weldline. The structure at the weldline cannot bear stress like the rest of the LCP structure and fails. The connected hierarchical structure in the 50% LCP blend has been observed through microscopy to be not as developed as that in the neat LCP. The undeveloped connected hierarchy is responsible for the low strength and strain at break in Figure 18, which is not significantly affected by the presence of a weldline. The properties in the 50% LCP blend with a weldline are similar to those without a weldline due to the entanglement of the PET in the blend at the juncture of the two flow fronts. The dependence of the modulus upon the LCP content for both samples with and without a weldline is seen in Figure 20. The dependence of the modulus on the LCP content in both cases is similar to what could be expected from an inverse rule of mixtures calculation. The presence of the weldline makes little difference in the initial stiffness of the blends.

The variation of the strength with LCP content in the blends exhibits a minimum strength between 25% and 75% LCP in Figure 21. The minimum in the strength is a direct result of the differences in the blend structure. The blends with 25% or more PET cannot draw due to the presence of the undrawable LCP domains. Between 25 and 75% LCP there is too much LCP to allow drawing, but, on the other hand, not enough LCP in a connected hierarchical structure to toughen the material. The

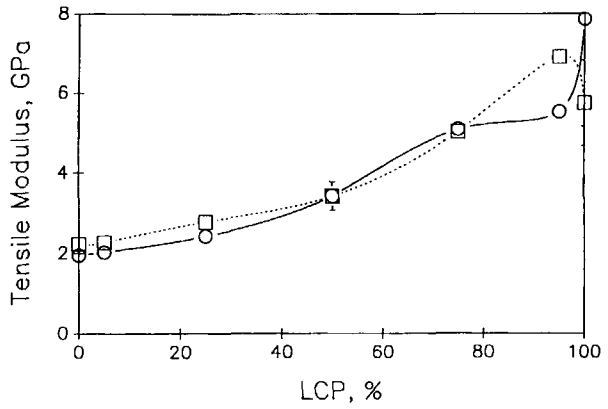

Figure 20 Variation of tensile modulus with blend composition: (O——O) no weldline; (□ - - - □) weldline.

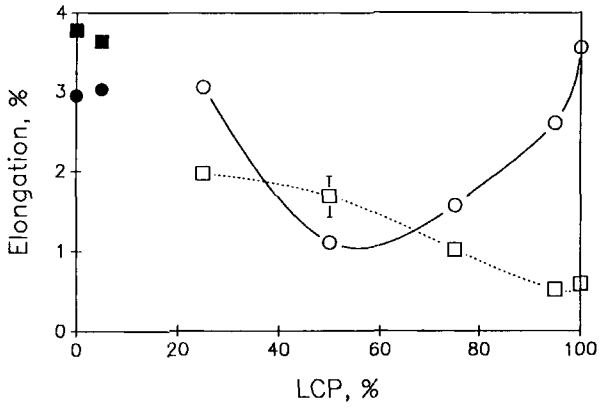

Figure 22 Variation of strain at break with blend composition: (O——O) no weldline; (□ - - - □) weldline. Yield strain: (●) no weldline; (■) weldline.

strength doubles between 75 and 95% LCP in the blends. Only at 95% LCP is there a structural similarity to neat LCP with a highly connected structure that makes the LCP woodlike and tough. The elongation at break of the blends in Figure 22 displays the same phenomenon with a minimum of elongation between 25 and 75% LCP due to the inability to draw on one hand, and the undeveloped connected hierarchy on the other. The LCP has a weak spot at the weldline due to the same disruption of the connected hierarchical structure found in the blends resulting from the presence of the PET. The large increase in mechanical properties from 75 to 95% LCP in Figures 20, 21, and 22 is due to their structural differences.

Impact Strength

The impact strengths in Figure 23 exhibits a minimum between 25 and 75% LCP similar to that found in the tensile tests. The smooth fracture surfaces in the blends with 75% or less PET are similar to that of PET. The impact strength, however, jumps 10-fold between 75 and 95% LCP due to the latter's LCP-like structure. The fracture surface of the LCP and 95% LCP blend is jagged, with the fracture propagating only halfway through the sample. The impact strength in the LCP and 95% LCP blend is also a function of the LCP orientation at the notch. The two points in Figure 23 for these compositions represent different distances between the notch and the injection inlet sprue and reflect the effect of the flow on orientation in the sample. The orientation of samples with a notch close to the inlet sprue is greater than those with the notch far from the inlet sprue. The impact strength at high LCP concentrations, which are more sensitive to orientation, is greater for the samples with the higher orientation.

The importance of orientation is seen as well in the tensile tests. The dependence of the properties

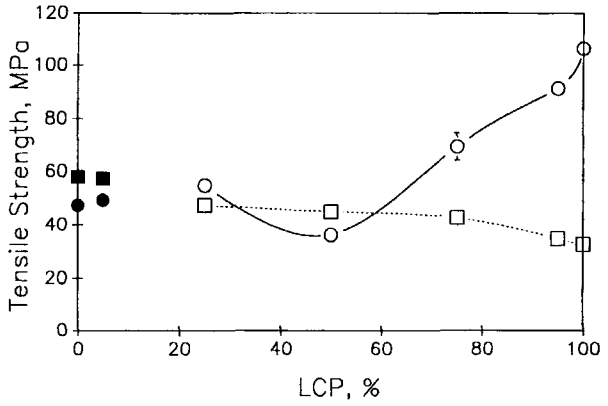

Figure 21 Variation of tensile strength with blend composition: (O——O) no weldline; (□ - - - □) weldline. Yield stress: (●) no weldline; (□) weldline.

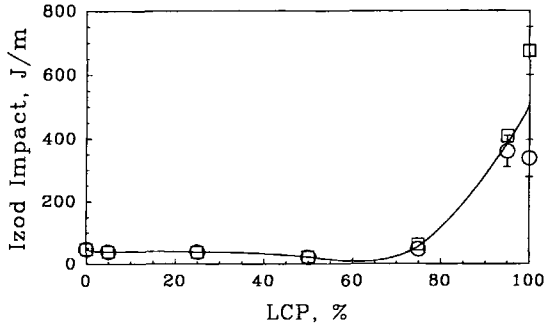

Figure 23 Variation of notched Izod impact energy with blend composition. Position of notch: (□) close to inlet sprue; (O) far from inlet sprue.

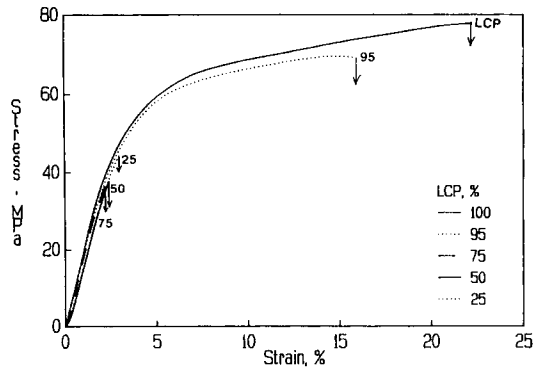

Figure 24 Stress-strain curves of 25, 50, 75, 95, and 100% LCP blends (strain rate 1%/min). Tested at an angle to the injection direction.

of the LCP and 95% LCP blend upon orientation distinguishes their connected hierarchical structure from that of the blends with 75% or less LCP. The stress–strain curves of specimens cut from an injection molded plaque and tested at an angle to the injection direction are seen in Figure 24. The blends with 25–75% LCP fracture in the same manner as those tested in the injection direction and exhibit similar properties. The LCP and blend with 95% LCP, however, exhibit a significant increase in elongation due to the angle between the applied stress and that of the highly oriented LCP structure.

CONCLUSIONS

1. Several levels of structural hierarchy can be distinguished in these blends of immiscible LCP and PET. The macroscopic core and skin, each 0.3 mm thick, have a gradient structure and can be subdivided into ordered and disordered sublayers between tens and hundreds of microns thick.
2. The sublayers contain rodlike LCP domains 2–5 μm in diameter at 25% LCP. The domains become thinner, longer, and more fibril-like with increasing LCP concentration. The interconnection between the LCP domains becomes more significant with increasing LCP concentration.
3. The LCP is highly oriented in the injection direction in the top layer with either a perpendicular orientation or with no discernable orientation at the sample center. This orientation reflects the elongational and fountain flow in the mold and increases with the LCP concentration.
4. The structure at 5% LCP is spherical LCP domains in a PET matrix and that at 95% LCP is spherical PET domains in an LCP matrix.
5. A minimum exists in the tensile strength, elongation at break and impact strength with varying blend composition at approximately 50% LCP. The tensile strength of the LCP rich blends is significantly lowered by the presence of a weldline or an angle between the stress and orientation directions. The unique mechanical properties of the LCP depends on the formation of a highly oriented and connected hierarchical structure that does not exist in blends with 75% or less LCP.

The authors gratefully acknowledge the fellowship and generous financial support of the Goodyear Tire and Rubber Co.

REFERENCES

1. M. G. Dobb and J. E. McIntyre, in *Advances in Polymer Science 60/61*, Springer-Verlag, Berlin, 1984, p. 61.
2. Y. Ide and Z. Ophir, *Polym. Eng. Sci.*, **23**, 261 (1983).
3. W. J. Jackson, Jr. and H. F. Kuhfuss, *J. Polym. Sci. Polym. Chem. Ed.*, **14**, 2043 (1976).
4. T. Weng, A. Hiltner, and E. Baer, *J. Mater. Sci.*, **21**, 744 (1986).
5. P. G. Hedmark, J. M. R. Lopez, M. Westdahl, P. E. Werner, J. F. Jansson, and U. W. Gedde, *Polym. Eng. Sci.*, **28**, 1248 (1988).
6. L. C. Sawyer and M. Jaffe, *J. Mater. Sci.*, **21**, 1897 (1986).
7. Z. Tadmor, *J. Appl. Polym. Sci.*, **18**, 1753 (1974).
8. Z. Ophir and Y. Ide, *Polym. Eng. Sci.*, **23**, 792 (1983).
9. T. Weng, A. Hiltner, and E. Baer, *J. Macromol. Sci. Chem.*, **A26**, 273 (1989).
10. T. Weng, A. Hiltner, and E. Baer, *J. Compos. Mater.*, **24**, 103 (1990).
11. A. Siegmann, A. Dagan, and S. Kenig, *Polymer*, **26**, 1325 (1985).
12. G. Kiss, *Polym. Eng. Sci.*, **27**, 410 (1987).
13. K. G. Blizard and D. G. Baird, *Polym. Eng. Sci.*, **27**, 653 (1987).

Received September 14, 1990
Accepted November 13, 1990